Available online at www.sciencedirect.com
SCIENCE DIRECT
Journal of Power Sources 146 (2005) 693–697
JOURNAL OF POWER SOURCES
www.elsevier.com/locate/jpowsour

Discharge–charge properties of Li/$LiCoO_2$ cell using room temperature ionic liquids (RTILs) based on quaternary ammonium cation – Effect of the structure

Hikari Sakaebe*, Hajime Matsumoto, Kuniaki Tatsumi

Research Institute for Ubiquitous Energy Devices, National Institute of Advanced Industrial Science and Technology (AIST) 1-8-31 Midorigaoka, Ikeda, Osaka 563-8577, Japan

Available online 27 April 2005

Abstract

The properties of the Li/$LiCoO_2$ cell containing several RTILs with three different anions were investigated. Introducing the asymmetric nature to anionic species using amide improved the viscosity and conductivity of the RTIL, however, the rate properties of the cell was not enhanced very much. Declined cathodic stability seems to be responsible for the result. In the case of the stable system consisting of quaternary ammonium cation and imide anion, both of cycling properties and Coulombic efficiency during the cycling were satisfactory and the viscosity dominated the rate properties of the cell. The performance of the Li/$LiCoO_2$ cell in this study was almost consistent with the stability of Li-electrolyte interface evaluated by ac impedance measurement.

Keywords: Room temperature ionic liquid; Quaternary ammonium; Symmetry of anion; Li battery; Interfacial stability

1. Introduction

Room temperature ionic liquid (RTIL) has attracted many researchers as a new solvent for electrochemical process in these days [1–7]. Due to the extremely low vapor pressure and the flame resistant properties, it is hoped that the use of RTIL for the electrolyte of lithium batteries would improve the safety of the battery.

One of the authors, Matsumoto, discovered the useful series with asymmetric quaternary ammonium cations, which enabled the reversible plating/stripping of lithium metal [8], and among them, authors have found a quite promising RTIL, *N*-methyl-*N*-propylpiperidinium bis(trifluoromethanesulfonyl)imide (PP13-TFSI, see Fig. 1). This novel RTIL showed the excellent properties in Li/$LiCoO_2$ cell [9]. The combination of cations and anions affected the cell properties, and we have reported the charge–discharge properties of Li/$LiCoO_2$ cell using several RTILs as the electrolyte. In this paper, some more kinds of RTILs with three different anions are tested and structure effect on the cell performance is discussed with rough classification of the anionic and cationic species.

2. Experimental

2.1. Preparation of RTIL

Cations and anions used for RTILs in this study are schematically described in Fig. 1 with abbreviations. In the case of the preparation of quaternary ammonium cation(QA)-TFSI RTIL, equimolar aqueous solution of QA-Br and LiTFSI (3M) was slowly mixed as described in the literature [8,9]. All the reagent for cation source was recrystallized. Moreover, the resulted RTIL was extracted and thoroughly washed by highly purified water. 1-ethyl-3-methylimidazolium(EMI)-TFSI was prepared according to the literature [10]. TSAC-based RTIL and C1C2-based RTIL were made from the halogenated cation with TSAC anion

* Corresponding author. Tel.: +81 72 751 7932; fax: +81 72 751 9609.
E-mail address: hikari.sakaebe@aist.go.jp (H. Sakaebe).

0378-7753/$ – see front matter © 2005 Elsevier B.V. All rights reserved.
doi:10.1016/j.jpowsour.2005.03.071

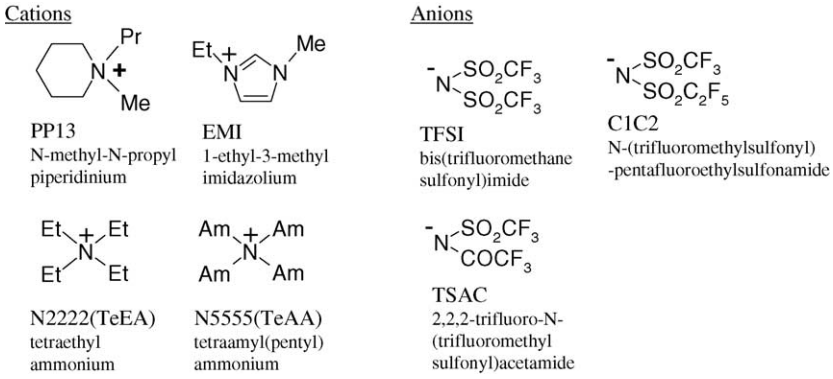

Fig. 1. Schematic illustrations of cationic and anionic species used in this study with their abbreviations.

provided from Tokuyama, Corp. and C1C2 anion provided from Central Glass Co. Ltd. using the similar technique. Matsumoto et al. have already observed that the purity of RTIL greatly affected the electrochemical properties [11]. Therefore the purity of RTIL was checked by X-ray fluorescence spectroscopy, inductively coupled plasma photoemission spectroscopy, chemical analysis, and so on. In order to prepare the electrolyte solution, each RTIL was vacuum-dried in the chamber placed inside the dry room with the due point between −80 to −50 °C. Then the 10 wt% of the supporting electrolyte LiTFSI (3M, recrystallized or highly purified reagent) which was dried separately in advance was added to the dried RTIL. This amount corresponds to 0.4 mol dm^{-3} in the case of PP13-TFSI. Almost all other RTIL (except for N5555-TFSI) had the density of 1.3–1.5 g cm^{-3} (Table 1 [12]) and thus the molar ratio does not deviate with each other very much.

2.2. Electrochemical measurement

Two-electrode cell sealed in Al-laminate film was used for the cycling test and ac impedance measurement in this study. The cell construction was carried out in the Ar-atomosphere glove box (due point was below −85 °C), and all the cell components except for Li were vacuum-dried before introduced in the glove box. For the cycling test of the lithium cell containing RTIL as an electrolyte base, lithium foil (99.9% as battery grade from Honjo Metal Co., 300 μm thickness) was used for a negative electrode. Positive electrode was fabricated by spreading the mixture of $LiCoO_2$ (Cell seed C5 from Nippon Chemical Industrial Co., Ltd.), acetylene black (Denka Black from DENKI KAGAKU KOGYO KABUSHIKI KAISYA), and PVdF (#1120 from Kureha Chemical Industry Co. Ltd.) with a weight ratio of 86:7:7 onto the Al current collector (battery use, 99.5% from Hosen). Loading of active material was ca. 1.0–1.5 mg cm^{-1} and roll-pressed to reduce the thickness to be 75%. Electrolyte solution was soaked into the separator (glass filter made of borosilicate glass, like GF/A from Whattman). Charge–discharge (C-D) cycling test of Li/$LiCoO_2$ cell was conducted galvanostatically using the Keisokuki C/D Unit 05-R1 and ASKA electronics Co. Ltd. ACD-003MA at the 0.1C–1C current rate. For ac impedance measurement cell, both of the working electrode and the counter electrode consisted of the Li foil (300 μm in thickness and 14 mm in diameter) pressed onto the Ni current corrector (Nilaco Co. Ltd. 99.7% 30 μm in thickness and 14 mm in diameter) directly connected to the tab. The separator was the same as the cell for the C-D cycling test. Potentiostatic ac impedance spectra was recorded using Solartron 1260 impedance analyzer and PARC potentiostat model 283. Cell voltage, ac amplitude, and frequency range was 0 V, 5 mV, and 1 MHz to 1 Hz, respectively. Temperature around cell was kept at 30 °C for first 2 weeks, then at 60 °C for succeeding 2 weeks.

3. Results and discussion

3.1. Prepared RTILs

By the careful preparation, obtained RTIL was colorless liquid with the higher purity. In all RTILs used in this study,

Table 1
Physical properties of RTILs used in this study [12]

Cation	Anion	MW	Density^{25} (g mL^{-1})	Viscosity at 25 °C (cP)	Conductivity at 25 °C (mS cm^{-1})
PP13	TSAC	386	1.37	98	2.1
PP13	TFSI	422	1.43	151	1.4
PP13	C1C2	472	1.46	281	0.71
N5555	TFSI	578	1.16	554	0.15
N2222	TFSI	374	1.37	60	3.6
EMI	TSAC	355	1.46	25	9.9
EMI	TFSI	391	1.52	33	8.7

content of water, haologenated impurity, alkali metal were less than 20 ppm, less than 15 ppm, below detection limit, respectively.

Physical properties and electrochemical stability of the several RTILs would be reported in the separated paper [12]. Here, physical properties of RTIL used in this study was summarized in Table 1. The order of the viscosity was; N5555-TFSI > PP13-C1C2 > PP13-TFSI > PP13-TSAC > EMI-TFSI > EMI-TSAC. RTIL with QA exhibited larger viscosity than those with EMI, and it was clear that using TSAC anion adding asymmetric nature, viscosity was improved. On the other hand, C1C2 anion made RTIL more viscous. Effect of increase in molecular weight might exceed the asymmetric effect in this case. Cathodic stability was in the order of; N5555-TFSI = PP13-TFSI > PP13C1C2 > PP13-TSAC = N2222-TSAC > EMI-TFSI > EMI-TSAC [12]. Unfortunately TSAC reduced the cathodic stability though improved the dynamic properties.

3.2. C-D properties of $Li/LiCoO_2$ cell containing typical RTILs

C-D properties seem to strongly depend on the electrochemical stability of RTILs. Cathodic stability in the previous section and linear sweep voltammogram [9] indicated that generally QA-TFSI based RTILs showed the sufficient stability for the Li-metal anode. Fig. 2 illustrates the 1st and the 20th C-D curves of $Li/LiCoO_2$ cell containing several RTILs. PP13-TFSI (Fig. 2(a)) revealed the excellent performance as already reported [9], and the cycling properties were slightly improved by applying the roll-pressing of the electrode. Fig. 2(b) and (d) provide the C-D curves for the cell containing EMI cation. Both of EMI-TFSI and EMI-TSAC had the poorer cathodic stability than ammonium-TFSI series of RTIL, and the C-D curves reflect it having larger irreversible capacity and more rapid capacity degradation, especially in the case of EMI-TSAC. On the other hand, exchanging the cation of EMI-TSAC with PP13 improved the cathodic stability [12], at the same time, C-D properties (Fig. 2(c)). These results are summarized in the discharge capacity change (Fig. 3) and the plot of Coulombic efficiency during cycling (Fig. 4). In Fig. 4, Coulombic efficiency of N5555-TFSI and PP13C1C2 was partly higher than 100 %. These RTILs were the most viscous among the RTIL used in this study (Table 1, [12]), and the viscosity could be partly responsible for this phenomenon. The viscosity effect could

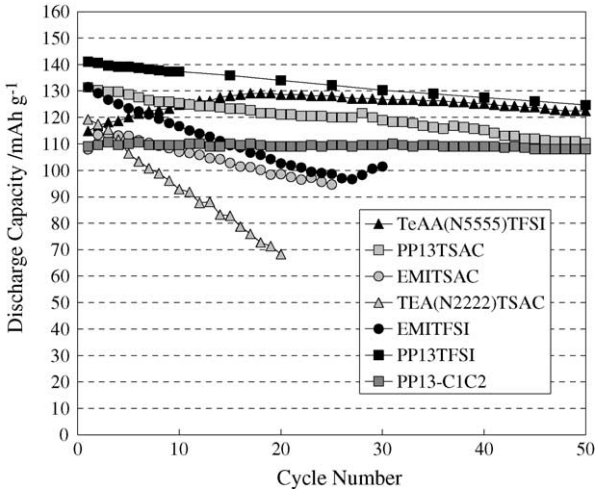

Fig. 3. Cycling properties during 50 cycles of the $Li/LiCoO_2$ cell containing 0.4 mol dm^{-3} LiTFSI in TeAA(N5555)-TFSI (closed triangle), 0.4 mol dm^{-3} LiTFSI in PP13-TSAC (light gray square), 0.4 mol dm^{-3} LiTFSI in EMI-TSAC (gray circle), 0.4 mol dm^{-3} LiTFSI in TeEA(N2222)-TSAC (gray triangle), 0.4 mol dm^{-3} LiTFSI in EMI-TFSI (closed circle), 0.4 mol dm^{-3} LiTFSI in PP13-TFSI (closed square), 0.4 mol dm^{-3} LiTFSI in PP13-C1C2 (dark gray square). Charge cut off: 4.2 V CC mode, discharge cut off: 3.2 V CC mode, charge and discharge current rate: *C*/10.

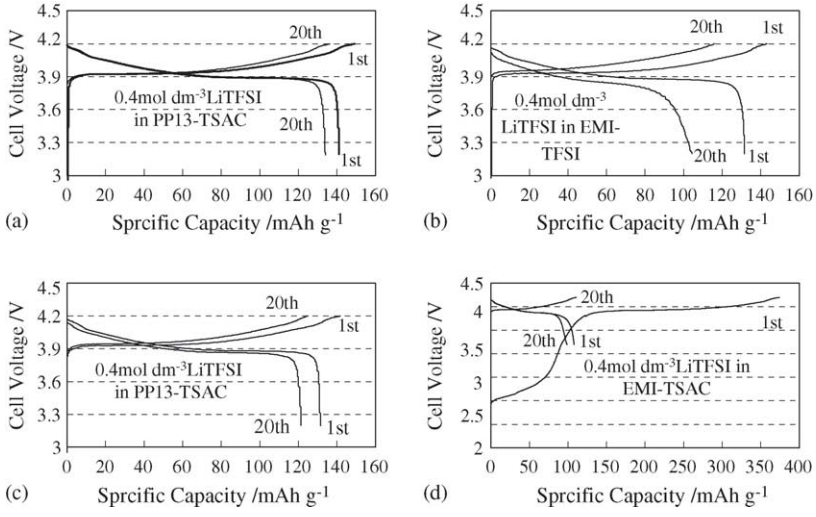

Fig. 2. First and 10th charge–discharge curves for $Li/LiCoO_2$ cell containing (a) 0.4 mol dm^{-3} LiTFSI in PP13-TFSI, (b) 0.4 mol dm^{-3} LiTFSI in EMI-TFSI, (c) 0.4 mol dm^{-3} LiTFSI in PP13-TSAC, (d) 0.4 mol dm^{-3} LiTFSI in EMI-TSAC. Charge cut off:4.2 V CC mode, discharge cut off: 3.2 V CC mode, charge and discharge current rate: *C*/10.

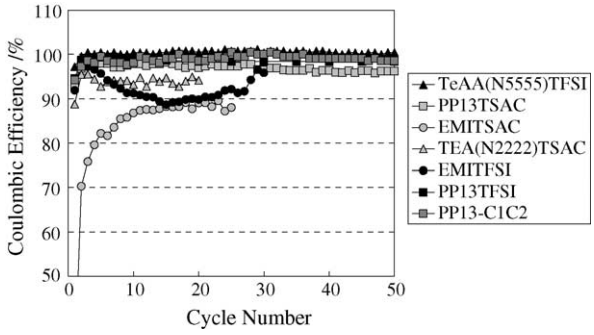

Fig. 4. Coulombic efficiency of charge and discharge during 50 cycles of the Li/$LiCoO_2$ cell containing 0.4 mol dm^{-3} LiTFSI in TeAA(N5555)-TFSI (closed triangle), 0.4 mol dm^{-3} LiTFSI in PP13-TSAC (light gray square), 0.4 mol dm^{-3} LiTFSI in EMI-TSAC (gray circle), 0.4 mol dm^{-3} LiTFSI in TeEA(N2222)-TSAC (gray triangle), 0.4 mol dm^{-3} LiTFSI in EMI-TFSI (closed circle), 0.4 mol dm^{-3} LiTFSI in PP13-TFSI (closed square), 0.4 mol dm^{-3} LiTFSI in PP13-C1C2 (dark gray square). Charge cut off:4.2 V CC mode, discharge cut off: 3.2 V CC mode, charge and discharge current rate: *C*/10.

be also observed in cycling properties (Fig. 3), where the discharge capacity was very stable and rather small for these two RTILs. The cell containing N5555-TFSI gradually increased the capacity during the initial 20 cycles with the slow penetration of electrolyte inside the electrode.

Fig. 5 shows the rate dependency of the discharge capacity of the cells containing several RTILs. Capacity was normalized against the first discharge capacity at the C/10 rate of the same cell. The cells could be classified into three groups. The first group contained RTILs with lower viscosity and poor cathodic stability, that is, EMI-TFSI, PP13-TSAC, and so on. The second group involved RTIL with higher viscosity and sufficient cathodic stability like PP13-TFSI. The difference in rate properties of first and second group was not significant

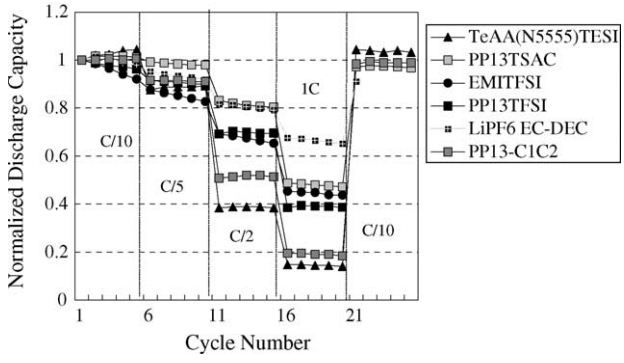

Fig. 5. Rate properties of the Li/$LiCoO_2$ cell containing 0.4 mol dm^{-3} LiTFSI in TeAA(N5555)-TFSI (closed triangle), 0.4 mol dm^{-3} LiTFSI in PP13-TSAC (light gray square), 0.4 mol dm^{-3} LiTFSI in EMI-TFSI (closed circle), 0.4 mol dm^{-3} LiTFSI in PP13-TFSI (closed square), 1.0 mol dm^{-3} $LiPF_6$ in EC-DEC (ethylene carbonate-diethyl carbonate) (white cross in closed square), 0.4 mol dm^{-3} LiTFSI in PP13-C1C2 (dark gray square). Charge cut off:4.2 V CC mode, discharge cut off: 3.2 V CC mode, charge and discharge current rate is shown in the figure. Discharge capacity was normalized using the first discharge capacity at the C/10 rate of the same cell.

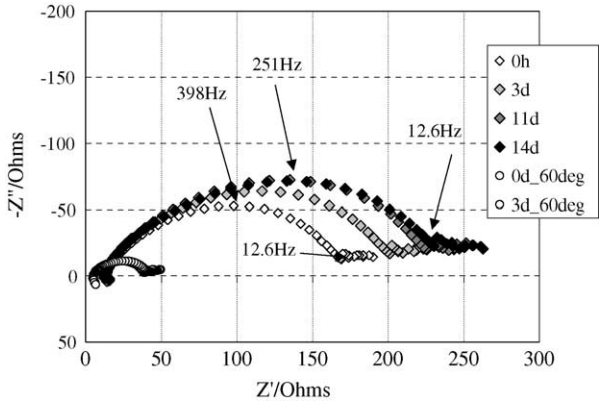

Fig. 6. ac impedance spectra (Nyquist plots) of the cell Li/0.4 mol dm^{-3} LiTFSI in PP13-TFSI /Li at 30 and 60 °C.

though the viscosity and conductivity differed considerably. The cell in the first group showed rapid degradation of the capacity (Fig. 3) and this was because they showed poor rate properties in the evaluation scheme in this study. RTIL with higher cathodic stability and further viscosity seemed to belong to the third group (N5555-TFSI and PP13C1C2) with the poor rate properties. From the results above, viscosity of RTILs basically dominate the rate dependency of the discharge capacity, however, it could be seen that the cathodic stability played an important roll in the rate capability of the cell.

3.3. *Interfacial stability between Li metal and electrolyte containing RTILs*

A lot of literature could be found concerning the results of ac impedance spectroscopy of Li-electrolyte interface [13–18], and this technique was used to estimate the stability of the surface film on the Li metal. Fig. 6 shows the time and temperature dependency of ac impedance spectra of Li/Li cell containing 0.4 mol dm^{-3} LiTFSI in PP13-TFSI. Each spectrum was shaped as a large depressed semicircle in the higher frequency region and with/without the line or a part of small semicircle, being very alike the one reported by Aurbach and Zaban [14]. They proposed the structure of the interface between Li and electrolyte could be modeled as a combination of the components with five different time constants. In this study, symmetric two-electrode cell was used and we did not dare to analyze precisely. Instead, the maximum value in the imaginary part of each impedance spectrum (R_{max}) was used to evaluate the time-dependency of the ohmic resistance of main component. This R_{max} value relatively corresponds to the resistance of the SEI layer on the Li metal [13–17]. Fig. 7 provides the R_{max}–time plot for the several RTIL. For neat PP13-TFSI, R_{max} showed the large value only at the beginning, and then decreased to be constant. After the temperature was raised up to 60 °C, total impedance dramatically decreased and gradually increased as the time. This result indicated that neat PP13-TFSI would form the

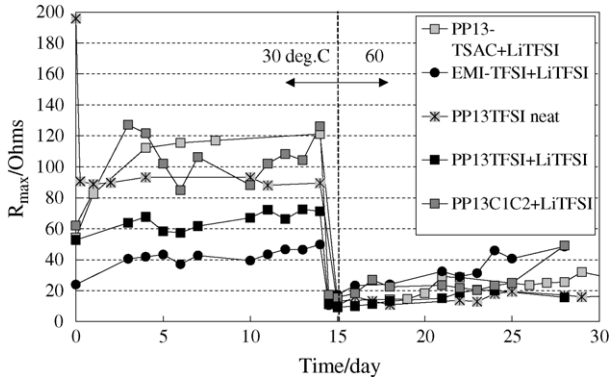

Fig. 7. Time dependence of the maximum value of imaginary part (R_{max}) of each impedance spectrum of the cell containing 0.4 mol dm^{-3} LiTFSI in PP13-TSAC (light gray square), 0.4 mol dm^{-3} LiTFSI in EMI-TFSI (closed circle), neat PP13-TFSI (star in gray square), 0.4 mol dm^{-3} LiTFSI in PP13-TFSI (closed square), 0.4 mol dm^{-3} LiTFSI in PP13-TFSI with 1000 ppm of H_2O added (open square), 0.4 mol dm^{-3} LiTFSI in PP13-C1C2 (dark gray square). Each cell was kept at 30 °C for the first 2 weeks and then temperature was raised to 60 °C in succeeding 2 weeks.

quite stable SEI (Solid Electrolyte Interface) layer on the Li. When LiTFSI was mixed, the R_{max} right after the construction of the cell was relatively small and then slightly increased but almost constant. At 60 °C, slowly R_{max} increased. This result implies that this electrolyte was rather stable against Li. On the other hand, R_{max} of the cell containing PP13-TSAC and PP13-C1C2 increased at the higher rate than PP13-TFSI. PP13-C1C2 had higher viscosity and it can be said that penetration of electrolyte into SEI layer would be partly responsible for R_{max} increase. PP13-TSAC showed much smaller viscosity and the increase in R_{max} would imply the SEI layer growth. For EMI-TFSI, R_{max} at 30 °C was rather small value probably reflecting the higher conductivity than QA system, but slowly increased. At 60 °C, more rapidly R_{max} increased. This increase in R_{max} also indicated that the SEI layer on Li grew as the time, implying that the RTILs would be more reactive with Li. In this sense, EMI-TFSI had initially lower R_{max}, however, was rather reactive with Li judging from the increasing rate of R_{max} at 60 °C. The RTIL stability against Li totally corresponded to the C-D properties of the Li/$LiCoO_2$ cell containing RTIL (Figs. 2–4).

4. Conclusion

Several RTILs with the high purity were prepared and it was confirmed that the combination of cationic and anionic species varies the physical properties and cathodic stability of RTIL. The variation in the viscosity, the conductivity and the electrochemical stability affected the C-D properties. The viscosity of the RTIL was dominant in the rate properties, however, cathodic stability was also responsible. The increasing rate of resistance of SEI layer reflected the RTILs stability against Li. C-D properties of the cell containing RTILs depended on this stability, too. Quite recently novel RTIL was found using the new anionic species [19]. Using the RTIL containing new anion, it may be hoped to exhibit the interesting cell performance in the Li battery system.

Acknowledgement

A part of this work was supported by the project concerning Li battery by NEDO and METI. Authors are also grateful for Tokuyama Corp. for the supply of TSAC anion source, and for Central Glass Co. Ltd. for supply of C1C2 anion source.

References

[1] N. Papageourgiou, Y. Athanassov, M. Armand, P. Bonhote, H. Pettersson, A. Azam, M. Gratzel, J. Electrochem. Soc. 143 (1996) 3099.
[2] T. Matsuda, H. Matsumoto, Electrochemistry 70 (2002) 446.
[3] V.R. Koch, L.A. Dominey, C. Nanjundiah, M.J. Ondrechen, J. Electrochem. Soc. 143 (1996) 798.
[4] Y.S. Fung, R.Q. Zhou, J. Power Sources 81 (1999) 891.
[5] H. Matsumoto, M. Yanagida, K. Tanimoto, T. Kojima, Y. Tamiya, Y. Miyazaki, Molten salts XII, In: P.C. Trulove, et al. (Eds.), Electrochem. Soc., Pennington, NJ (2000) 186.
[6] H. Nakagawa, S. Izuchi, K. Kuwana, T. Nukuda, Y. Aihara, J. Electrochem. Soc. 150 (2003) 695.
[7] T. Sato, G. Masuda, K. Takagi, Electrochim. Acta 49 (2004) 3603.
[8] H. Matsumoto, Y. Miyazaki, Chem. Lett. (2000) 922.
[9] H. Sakaebe, H. Matsumoto, Electrochem. Commun. 5 (2003) 594–598.
[10] P. Bonhote, A-P. Dias, N. Papageourgiou, K. Kalyanasundaram, M. Gratzel, Inorg. Chem. 35 (1996) 1168.
[11] H. Matsumoto, H. Kageyama, Y. Miyazaki, Electrochemistry 71 (2003) 1058.
[12] H. Matsumoto, et al., J. Power Sources 146 (2005) 45–50.
[13] D. Aurbach, A. Zaban, J. Electroanal. Chem. 348 (1993) 155.
[14] D. Aurbach, A. Zaban, J. Electroanal. Chem. 367 (1994) 15.
[15] D. Aurbach, A. Zaban, J. Electroanal. Chem. 365 (1994) 41.
[16] K. Naoi, M. Mori, Y. Naruoka, W.M. Lamanna, R. Atanasoski, J. Electrochem. Soc. 146 (1999) 462.
[17] H. Ohta, K. Shima, M. Ue, J.-I. Yamaki, Electrochim. Acta 49 (2004) 565.
[18] J.-H. Shin, S. Passerini, Electrochim. Acta 49 (2004) 1605.
[19] Z.-B. Zhou, H. Matsumoto, K. Tatsumi, Chem. Lett. (2004) 886.